AD-A104 734 DEFENCE RESEARCH ESTABLISHMENT VALCARTIER (QUEBEC) F/G 20/5
A STARK CELL FOR FREQUENCY CONTROL OF A WAVEGUIDE CO2 LASER (U)
FEB 81 P LAVIGNE, A DESLAURIERS, J LEMAY

UNCLASSIFIED DREV-R-4188/81 NL

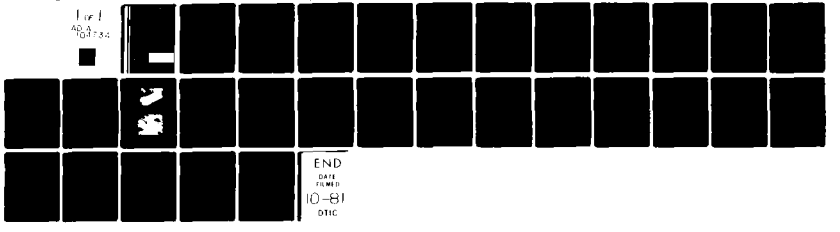

UNCLASSIFIED
UNLIMITED DISTRIBUTION

LEVEL II

(6)

CRDV R-REPORT-4136-81
DCIEM PROJECT 36331-004
REVISED 1981

CRDV R-REPORT-4136-81
DCIEM PROJECT 36331-004
REVISED 1981

AD A104734

A STARK CELL FOR FREQUENCY CONTROL OF A WAVEGUIDE CO_2 LASER

P. Lavigne

A. Deslauriers

J. Lemay

Centre de Recherches pour la Défense
Defence Research Establishment
Valcartier, Québec

BUREAU - RECHERCHE ET DEVELOPPEMENT
MINISTERE DE LA DEFENSE NATIONALE
CANADA

RESEARCH AND DEVELOPMENT BRANCH
DEPARTMENT OF NATIONAL DEFENCE
CANADA

UNCLASSIFIED WITHOUT ENCLOSURE

REPORT NO: DREV REPORT 4188/81

TITLE: A STARK CELL FOR FREQUENCY CONTROL OF A WAVEGUIDE CO2 LASER

DATE: FEBRUARY 1981

AUTHORS: P. Lavigne A. Deslauriers J. Lemay

SECURITY GRADING: UNCLASSIFIED

Distribution
1- Report Collection
1-Microfiche Section (unbound copy)
1-[illegible]
1-DREO
[illegible]DR
1-[illegible]DR
1-[illegible] Library
[illegible]
[illegible] Library
[illegible]
[illegible]

-[illegible] Library
1-[illegible]
1-[illegible]
1-[illegible]
1-D[illegible]
1-[illegible] Library for Micromedia Ltd.

BRITAIN
Ministry of Defence
3-DRIC

UNITED STATES
3-US Army Research Dev. Stand. Groups
3-DTIC/NTIS

Commonwealth
-Australia
3-Senior Army Standardization Representative, Ottawa
1-One hard copy and one microfiche copy report (as they become available) to:
Department of Defence
Campbell Park Offices
Canberra A.C.T. 2600
Australia
Attn: Defence Information Services Branch

3-New Zealand
1-Defence Scientific Establishment

NATO
2-[illegible]
1-[illegible]
1-[illegible]
[illegible]
[illegible] 1-Head, [illegible]
[illegible]

1-West Germany
4-Netherlands
1-Dutch Defence Est.
2-Norway
-Norwegian Def. Res. Est.
3-Turkey
1-Director, Res.&Dev. [illegible]
of Defence
1-[illegible] Tech. Center (if [illegible])

CRDV R-4188/81
DOSSIER: 3633H-004

UNCLASSIFIED

DREV-R-4188/81
FILE: 3633H-004

A STARK CELL FOR FREQUENCY CONTROL OF A WAVEGUIDE CO_2 LASER

(Une Cellule de Stark pour Controler la Frequence d'un Laser CO2 a Guide d'Ondes),

by

P. Lavigne, A. Deslauriers and J. Lemay

CENTRE DE RECHERCHES POUR LA DEFENSE
DEFENCE RESEARCH ESTABLISHMENT
VALCARTIER
Tel: (418) 844-4271

Québec, Canada

February/février 1981

NON CLASSIFIE

RESUME

Dans ce rapport, nous décrivons le mode d'opération et les détails de construction d'une cellule à effet Stark, susceptible de contrôler la fréquence d'un oscillateur local à 10 µm, et nous en analysons les caractéristiques. Avec cette cellule, nous avons réussi à syntoniser un laser CO_2 continu à guide d'ondes dans un domaine de fréquence de ± 100 MHz autour du centre de la raie P(20) du CO_2, à 10.6 µm, et nous avons obtenu une stabilité à long terme supérieure à ± 1.5 MHz. (NC)

ABSTRACT

In this report, we describe the mode of operation and the design of a Stark cell suitable for the frequency control of a local oscillator at 10 µm, and we analyze its characteristics. Using this cell, a waveguide CW CO_2 laser was tuned over ± 100 MHz around the line center of the P(20) CO_2 line, at 10.6 µm, and a long-term frequency stability better than ± 1.5 MHz was achieved. (U)

TABLE OF CONTENTS

1.0 INTRODUCTION

There is a need for a tunable, frequency-stabilized, CO_2 local oscillator for heterodyne detection at 10 μm. The possibility of setting the local oscillator frequency at some intermediate frequency, with respect to the line center, without dithering it, also appears desirable to fully benefit of the advantages of heterodyne detection. Recently, Nussmeier and Abrams (Ref. 1) described a new technique to lock the frequency of a CO_2 laser with an external gas cell whose resonant frequency is controlled by the linear Stark effect. This versatile technique allows both to eliminate the troublesome frequency modulation of the laser output and to tune the emission frequency.

The purpose of this report is to describe the principles of operation of the Stark cell stabilizing technique, to outline the design of a rugged, reliable and compact Stark cell as well as to analyze its performances. This work was performed at DREV between January 1978 and December 1979, under PCN 33H04, Miniaturization of Lasers.

2.0 MODE OF OPERATION

In the most basic configuration, the frequency of a CO_2 laser is controlled by a cell filled with a gas showing the Stark effect placed in the output beam of the laser. The resonance of the absorbing gas is tuned into coincidence with the desired laser frequency by using a dc electric field, as shown in Fig. 1. An increasing absorption then results in a decreasing transmitted signal. A modulation of a few volts, superimposed to the dc field, creates a dithering of the resonance about the laser frequency and leads to an amplitude modulation of the output. Coherent detection of this modulation gives a dc signal that is proportional to the slope of the transmission versus voltage curve. Consequently, an error signal is available that can be used

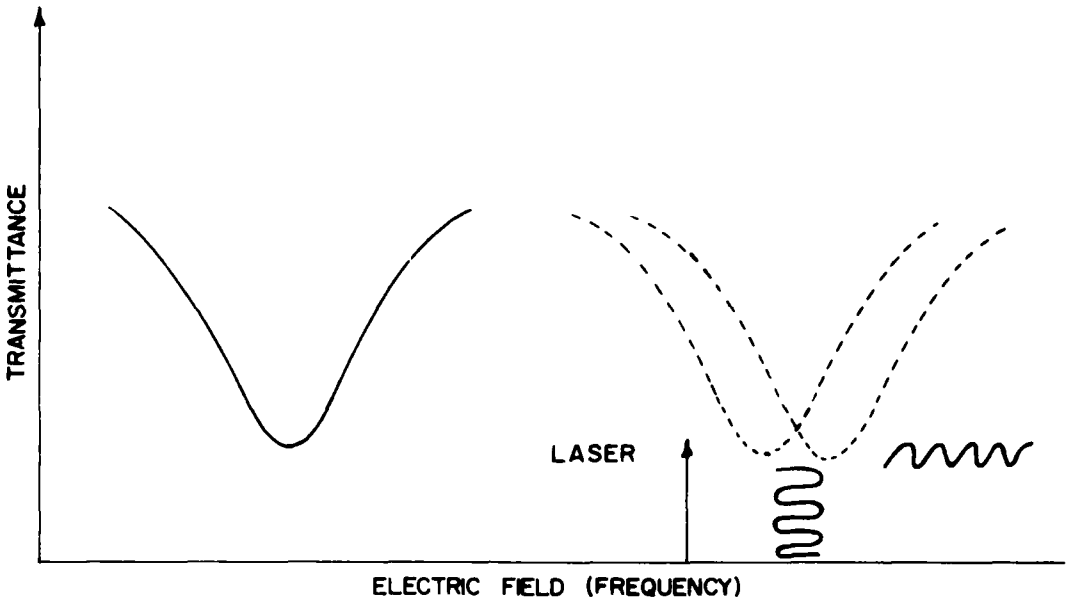

FIGURE 1 - Frequency stabilization and tuning of a laser utilizing the resonant absorption by a molecule with the Stark effect

in a servo-loop to lock the laser frequency to the center of the absorption line through appropriate cavity length correction with a bimorph or a PZT translator. This provides a laser frequency control function that can be easily implemented without having to FM modulate the laser frequency. It also improves the tunability, as any change in the dc field results in a tuning of the resonant frequency and, consequently, a tuning of the laser frequency.

Most of the CO_2 lasers used in optical radars or communications lase on the P(20) line of the 10.4 μm branch, which is the strongest CO_2 laser line. Many molecules (Refs. 2,3) exhibiting Stark effect have absorption characteristics at frequencies only a few megahertz distant from the CO_2 P(20) line. Usually, these absorption lines are very weak and they are not appropriate to the construction of a compact cell because a high-modulation index requires a very long interaction path. Fortunately, NH_2D has a resonant high-absorption line close to the CO_2 P(20) line that exhibits a linear Stark effect (Ref. 4). The interaction levels have been identified as $(0_a\ 4_{04}) \rightarrow (1_a\ 5_{05})$ (Ref. 5). They are illustrated in Fig. 2. Even if NH_2D is an asymmetric top molecule, a first-order Stark effect results from the near degeneracy of the lower level with the $(0_s\ 4_{14})$ level (Ref. 5). Consequently, this latter level is strongly coupled with the $(0_a\ 4_{04})$ level by an electric field.

In the high field limit, the resonant absorption frequency δ, relative to the P(20) line center of the CO_2, is given by the relation (Ref. 1):

$$\delta = -2042 + 0.143\ |M|E \qquad [1]$$

where δ is expressed in MHz, M is the Z component of J and can take integer values from -4 and +4 (-M and +M are degenerate) and E is the electric field in V/cm. At high pressure ($p \gtrsim 5$ torr), in the homogeneous line broadening regime, the limit of the line center absorption coefficient of the $|M| = 4$ transition is found to be 0.028 cm^{-1} (Ref. 6). At room temperature, the theoretical Doppler width (FWHM) amounts to 82 MHz, whereas the high pressure broadening rate

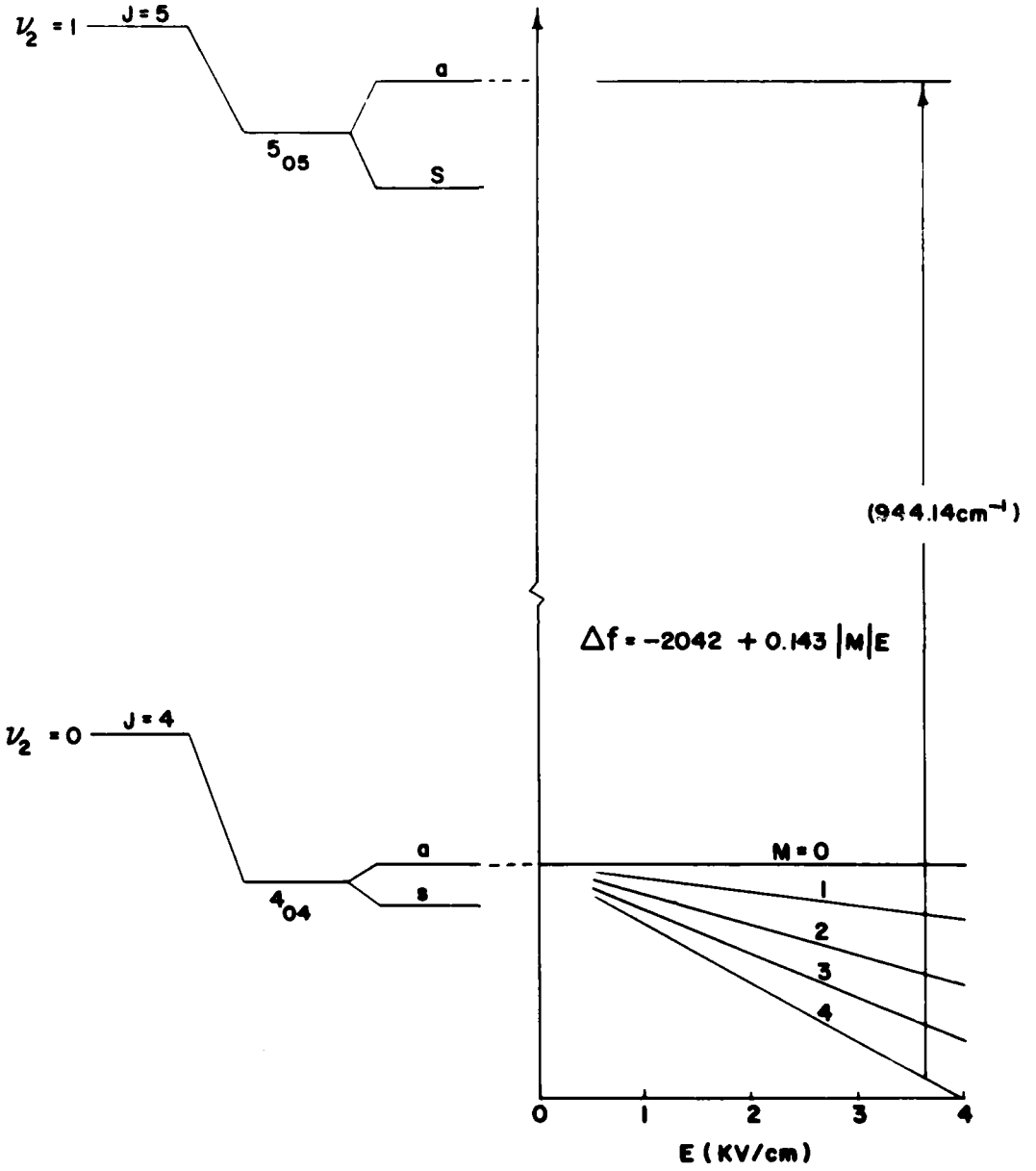

FIGURE 2 - Energy levels of NH_2D relevant to the frequency stabilization of a CO_2 laser on the P(20) line

is 40.2 MHz/torr (Ref. 6). Selection rules require that the electric field be perpendicular to the optical field direction for transitions with $\Delta M = \pm 1$. Equation [1] shows that the absorption line center can be displaced relatively to the P(20) line center so that a tunable reference is available to stabilize and tune the P(20) line of a CO_2 laser.

Using NH_2D, strong resonant absorption with Stark effet is not only found with the P(20) line, but also at frequencies close to those of the R(12) and P(14) lines of the 10-μm band of CO_2 (Ref. 7). This implies that the same Stark cell can be used to lock and stabilize a CO_2 laser on these lines. These possibilities are more numerous in natural CO_2 with the strong absorption of $N^{15}H_2D$ close to the R(18) and P(26) lines of CO_2, and with the medium absorption of either $N^{15}H_2D$ or $N^{15}HD_2$, near the CO_2 P(10) and P(28) lines (Ref. 7). Furthermore, the very strong absorption of $N^{14}H_3$ (Ref. 8) can be used with the $C^{13}O_2{}^{16}$ laser R(18) line.

3.0 DESIGN AND CONSTRUCTION

3.1 Mechanical Design

An exploded view of the Stark cell is shown in Fig. 3. The vacuum envelope is made of a 1-mm-thick, 72-mm-long, 25-mm OD stainless steel tube. This tube is closed at one end by a stainless steel cover sealed with an O-ring. This cover supports a concentrically mounted 12-mm ZnSe window AR-coated on both sides. Two vacuum-tight feedthroughs allow electrical connections to the electrodes. A miniaturized stainless steel valve is brazed at the other end of the tube for quick filling of the cell. Another 12-mm, AR-coated, ZnSe window is fastened to the valve body to transmit the infrared radiation through the cell. The overall dimensions of the cell are 30 x 95 mm.

The electrode structure is made of two 1-mm-thick, 65-mm-long, stainless steel plates polished on the inner side. Since any inhomogeneity of the electric field results in a broadening of the absorption line and, consequently, in a reduction of the slope of the error signal versus displacement frequency curve, good parallelism of the electrode plates, which are held apart by 1-mm-thick flat alumina plates, must be very carefully insured. Four teflon screws hold the electrode assembly together. Experiments have indicated that the long-term stability of the electric field depends on the spacer material. The use of microscope plate spacers resulted in a long-term drift of the voltage required to tune the absorption line with the line center of the laser, while quartz and alumina spacers gave a good stability.

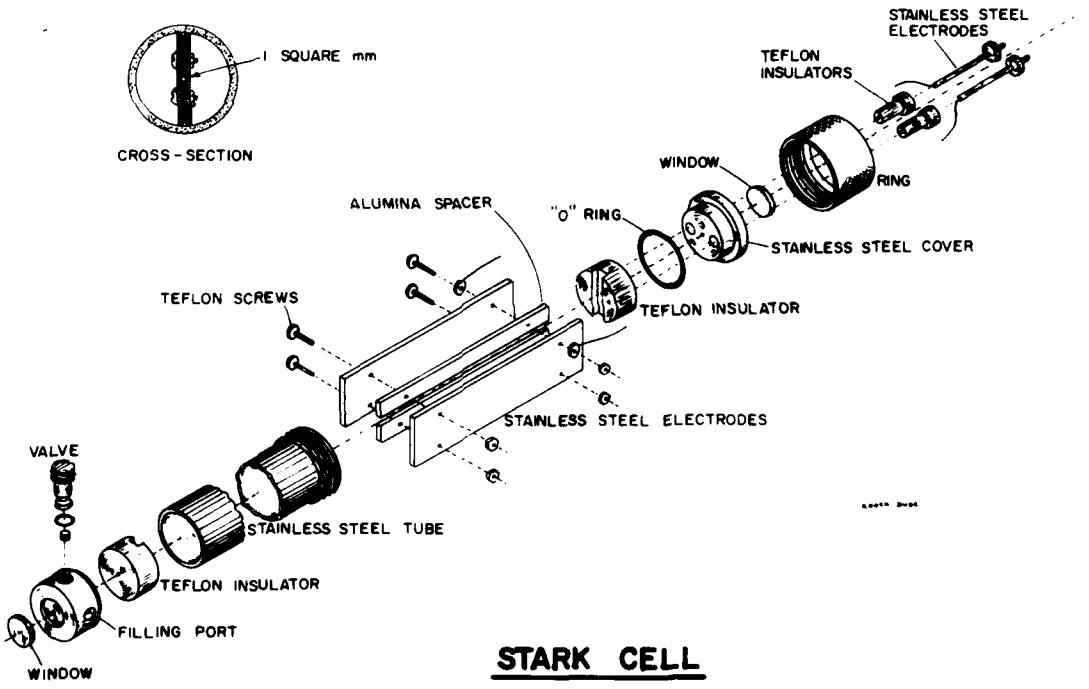

FIGURE 3 - Exploded view of the Stark cell assembly

At high pressure, with the 65-mm interaction length, a maximum absorption of 14% should be possible for the J = 4 transition. To apply the necessary electrical field of about 3600 V/cm at a sufficiently low pressure so as to have a steep discrimination curve without reaching the breakdown voltage, the interelectrode gap was set at 1 mm. As the spark-breakdown voltage curve, or Paschen curve, of NH_3, closely follows the curve of the air (Ref. 9), the spark-breakdown voltage should increase as the pressure decreases, starting at about 4 torr for a 1-mm gap.

3.2 Electronics

The detector used at the Stark cell output is a pyroelectric infrared detector (Molectron P1-40) mounted in a TO-99 case with a wideband, high input impedance operational amplifier. This detector can withstand a maximum average input power of 50 mW. With a feedback resistor of 10^9 Ω, its responsivity reaches about 10^3 V/W, with a 3-dB cutoff frequency of 1 kHz. The detector, a 10X voltage gain preamplifier, and a line driver are mounted on a printed circuit board and incorporated in a box fixed at the output of the Stark cell. Two voltage regulators are added to filter out any ripple or fluctuation of the ± 15-V supply voltage. Figure 4a illustrates the circuit used. A coaxial cable and two isolated wires are utilized to acquire the detector signal and supply the dc bias voltages.

The power source employed to apply the dc voltage required to tune the absorption line of NH_2D to the P(20) line of CO_2 is a precision photomultiplier power supply module (Bertan, model PMT-20 A) with a 0.001% load and line regulation, a 0.02% stability on an 8-hour run, and a $10^{-4}/^{o}C$ temperature coefficient. According to eq. [1], the best frequency stability is related as follows to the Stark electric field:

$$\frac{\Delta E}{\Delta \delta \ E} = 0.05\% \ \text{MHz}^{-1},$$

so that a long-term frequency stability of 400 kHz should be achievable with a proper servo-loop design. As shown in Fig. 4b, a 1-K trimpot, a 200-Ω, 10-turn calibrated potentiometer, and a 3.7-kΩ resistor are connected between pins 1 and 10 while the calibrated potentiometer wiper is connected to pin 8 for remote programming of the voltage. The trimpot is used to determine the center operating voltage and to limit the applied field to about 500 V and thus prevent an accidental breakdown in the Stark cell. The 200-Ω calibrated potentiometer allows a tuning range of 80 V, which represents about 400 MHz with a 1-mm gap. The modulation is superimposed to the dc voltage with a miniature transformer (Hammond 101D) which has a frequency response spanning the 200-50 kHz domain. Since the isolation of the transformer only amounts to 250 V, it is connected to the ground electrode of the Stark cell. The coupling transformer and the power module are mounted in a separate box and the modulated bias is brought to the Stark cell housing by two insulated wires. Figures 5a and b illustrate the Stark cell and the electrode assembly.

4.0 CELL CHARACTERISTICS

4.1 Breakdown Voltage

The breakdown voltage is an important parameter of the Stark cell as it limits the useful pressure range at which a cell can be operated. To have an idea of the voltage characteristics of the cell, a Paschen diagram was plotted; it is shown in Fig. 6. For this experiment, the cell was filled with a mixture of 50% NH_3 and 50% ND_3 (Ref. 10). As expected, because of the similarity with the air (Ref. 9), a maximum breakdown voltage of about 500 V was measured at a critical p × d value in the 4-5 torr-mm range. Since a voltage of

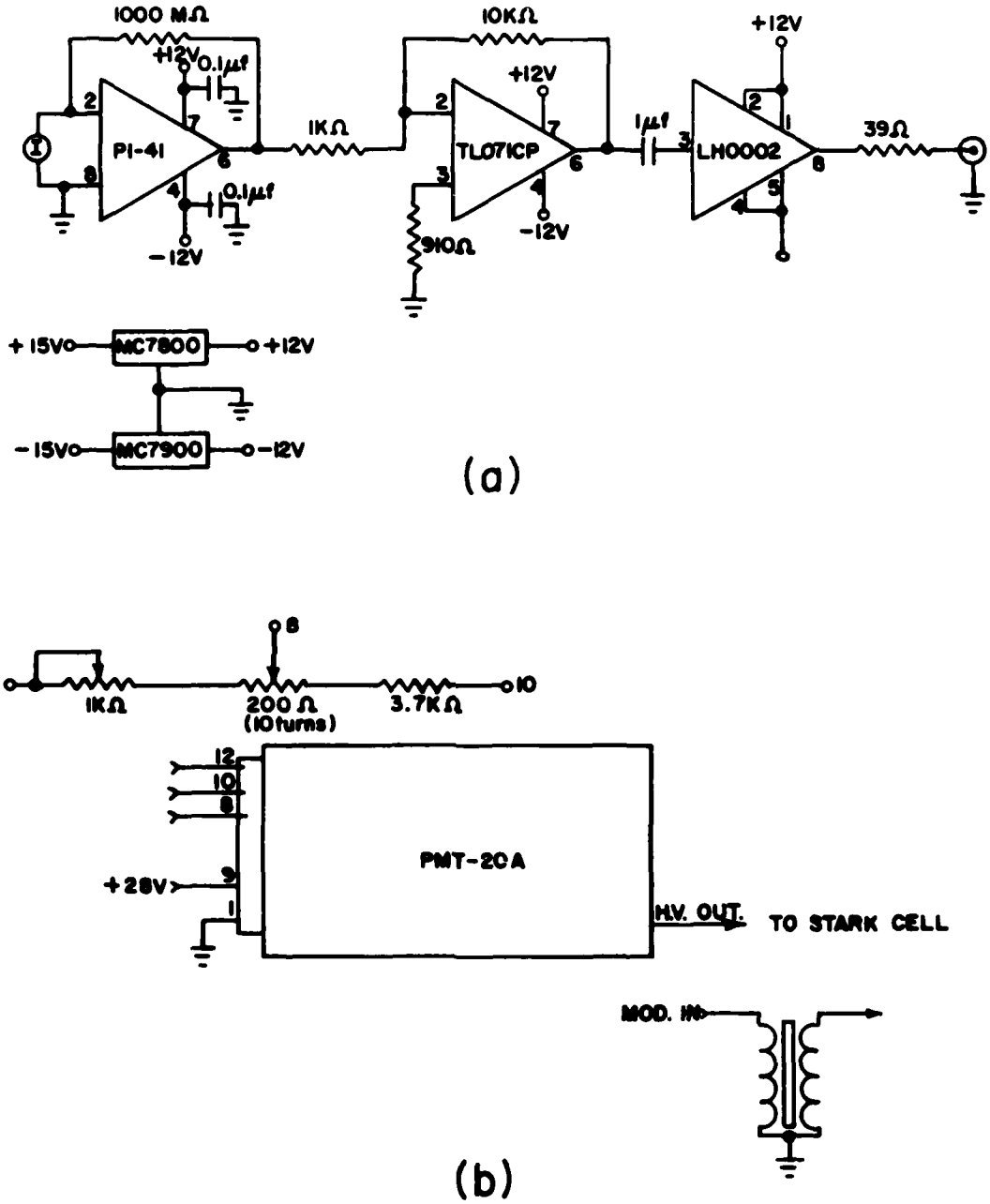

FIGURE 4 - Schematic circuit diagram of the accompanying electronic: (a) detector and preamplifier, (b) biasing circuit

(a)

(b)

FIGURE 5 - Photograph of the Stark cell and the electrode assembly

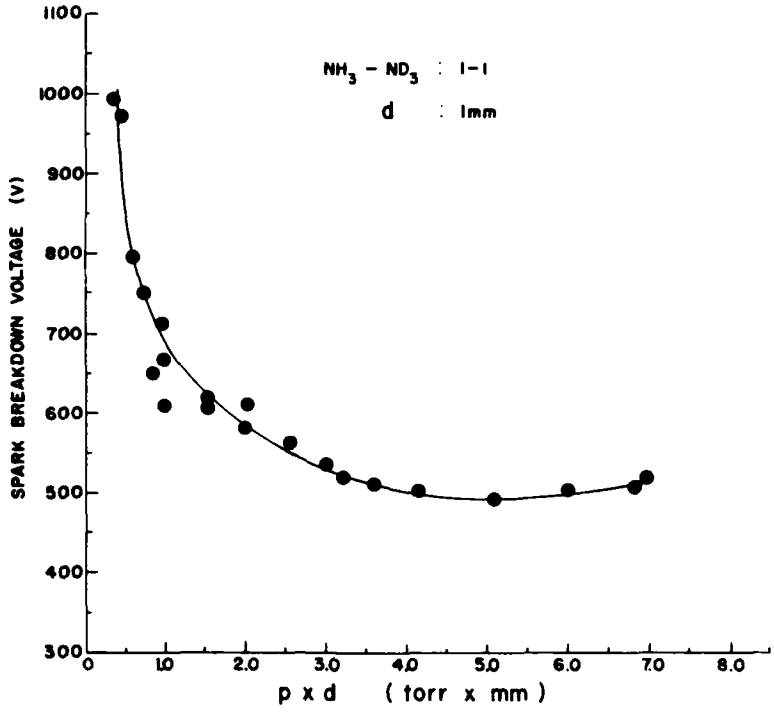

FIGURE 6 - Paschen curve for the Stark cell. The electrode spacing was about 1 mm.

about 360 V is required to bring the absorption profile of the $|M| = 4$ component into coincidence with the P(20) 10.4 μm line, the breakdown voltage does not limit the filling pressure when the gap is 1 mm wide. However, a study of the $|M| = 3, 2, 1$ components, which necessitate dc voltages of the order of 475, 715 and 1450 respectively, would require lower filling pressures or smaller gaps. For the application considered, that is the frequency tuning and stabilization of a CO_2 laser, the coincidence of the $|M| = 4$ component is sufficient and even desired because that transition exhibits the strongest frequency dependence.

4.2 Modulation Characteristics

Another important parameter of the cell is the absolute ac modulation depth resulting from a modulation of the applied field around a dc operating point. The modulation characteristics were measured with a low pressure CW CO_2 laser dither-stabilized within 1.5 MHz to the line center as a probe. In a first experiment, we measured the variation of the error signal in relation with the pressure. For this measurement, the probe laser, which sent 20 mW into the Stark cell, was tuned to the P(20) line center and a modulation signal of 2 V (peak-to-peak) at 530 Hz was applied to the Stark electrodes together with a 500-V linear ramp. The output of the cell was connected to a lock-in amplifier whose reference input was driven by the same 530-Hz signal as the Stark cell. When the output of the lock-in was plotted against the ramp signal, a discrimination curve resulted which represented the slope of the absorption. Figure 7 illustrates such a curve obtained when the cell pressure was 4 torr. The first and third zero-crossing points represent the voltage required to bring the $|M| = 4$ and $|M| = 3$ absorption lines of NH_2D respectively into coincidence with the P(20) CO_2 line. In the particular cell used, this voltage amounted to 375 V for the $|M| = 4$ transition. This indicates that the gap was somewhat larger than 1 mm.

Since it gives the rate of variation of the error signal with the offset frequency, the slope of the discrimination curve around the zero-crossing point represents a good means of evaluating the cell performance. The variation of this slope with the pressure is illustrated in Fig. 8. At low pressures, the slope increases following the absorption coefficient while the line is Doppler broadened.

At high pressures, the slope decreases consequently to a pressure broadening of the absorbing line and a constant absorption coefficient at the line center. The optimum pressure appears in the 2-2.5 torr region where the Doppler and the homogeneous linewidths are approximately equal. Further measurements were conducted at this optimum pressure of 2.5 torr.

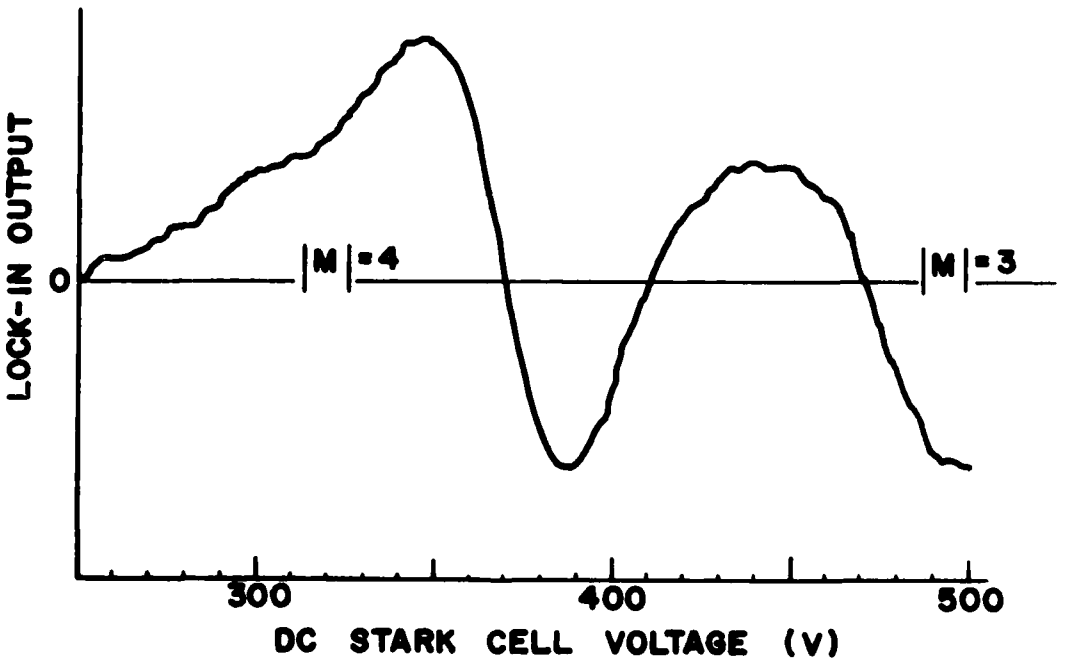

FIGURE 7 - Discrimination curve at 4 torr. The modulation voltage was 2 V p-p and the electrode spacing about 1 mm.

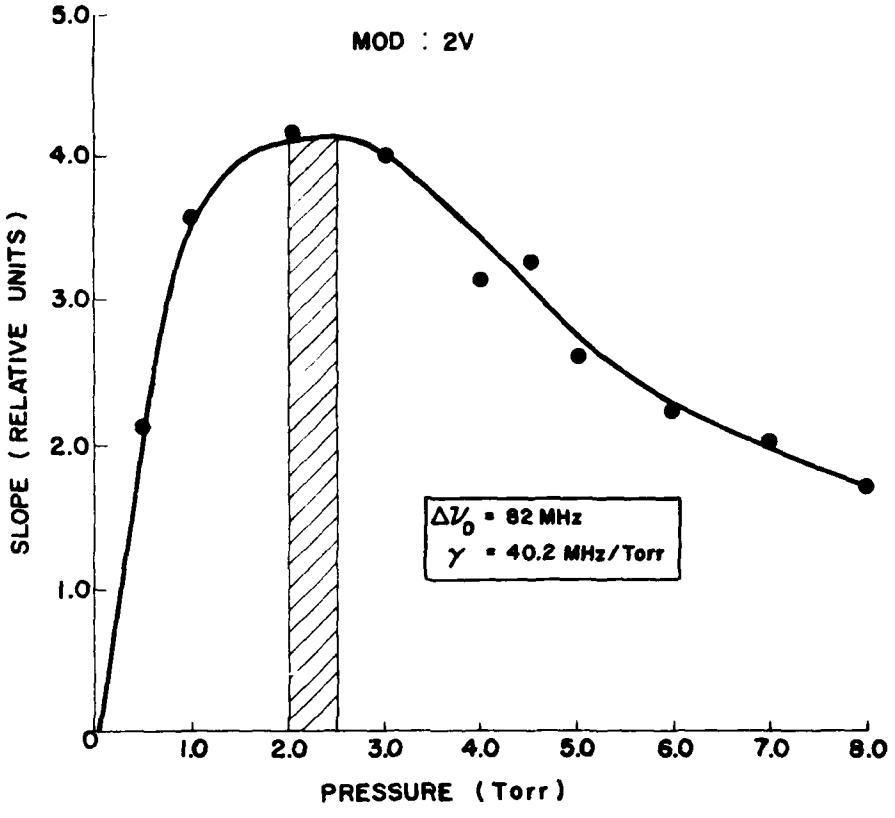

FIGURE 8 - Variation of the slope of the discrimination curve with the pressure, at the zero crossing point.

The modulation depth as a function of the modulating voltage amplitude is another feature of the cell. This was directly measured from the oscilloscope traces of both the driving and the output signals. The results are plotted in Fig. 9. For these measurements, the operating point was fixed at 361 V, where the modulation is higher. The output modulation increases linearly up to about 15 V with the driving voltage. At a higher drive, distortion occurs because of the nonlinearity of the absorption curve slope and of the saturation of the driving transformer.

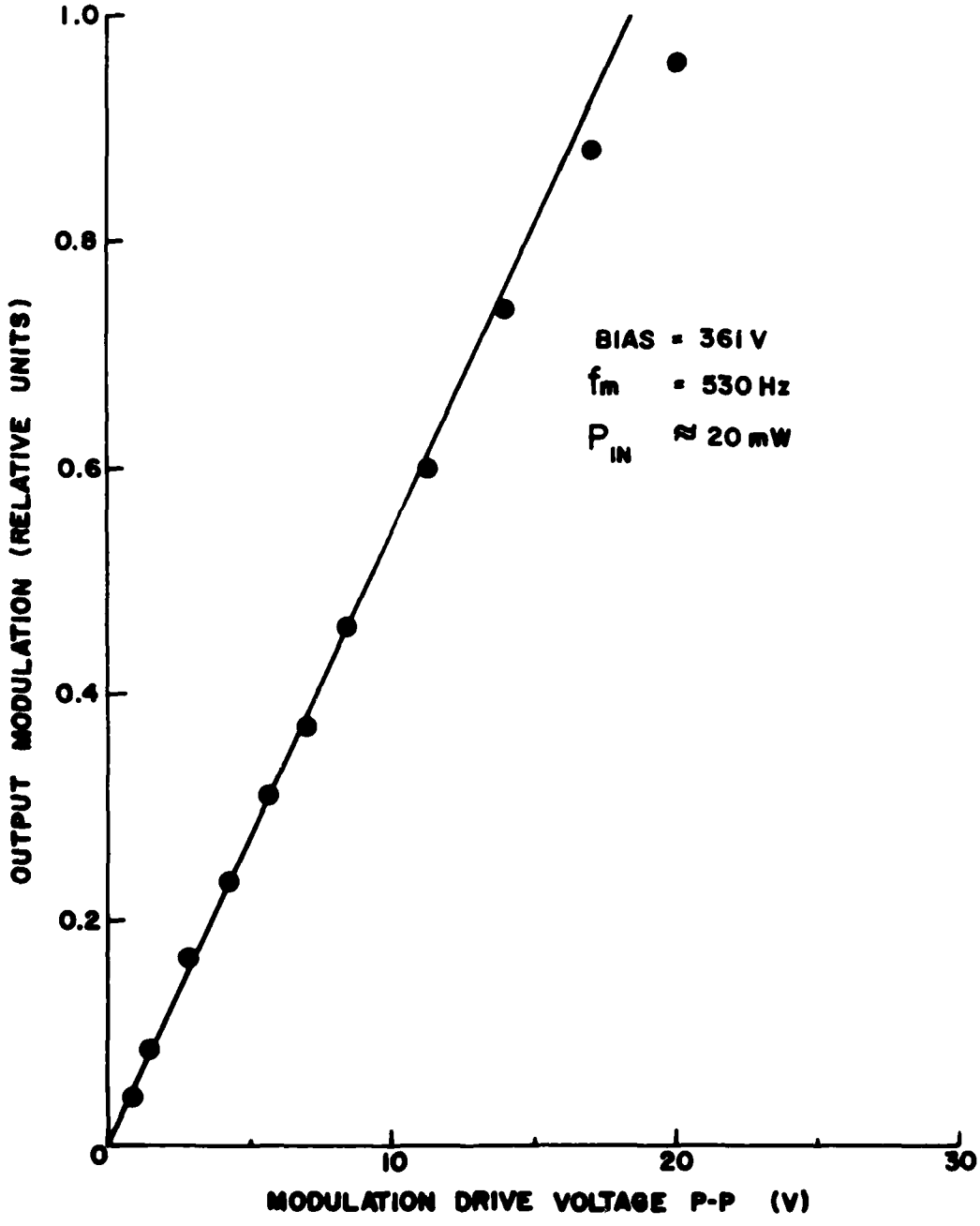

FIGURE 9 - Output modulation versus input modulation. The cell pressu e was 2.5 torr. The bias voltage was chosen to maximize the modulation. The circles indicate the accuracy of the measurements.

The frequency response of the cell at 2.5 torr, with a modulation voltage of 8 V, is shown in Fig. 10. This curve illustrates the limiting features of the electronic circuits more than the fundamental limitations of the cell. At frequencies lower than 100 Hz, the driving transformer severely distorts the driving signal. If necessary, this could easily be overcome by driving the lower potential electrode directly with the signal generator. The high frequency portion of the curve shows a 1/f falloff consistent with the capacitive nature of the detector. This portion can also be extended, with a corresponding decrease in sensitivity, by using a lower feedback resistor in the detector amplifier. The actual electronic circuit is suitable around 500 Hz, as planned, but a change in the operating frequency may require an appropriate change in the electronic circuit.

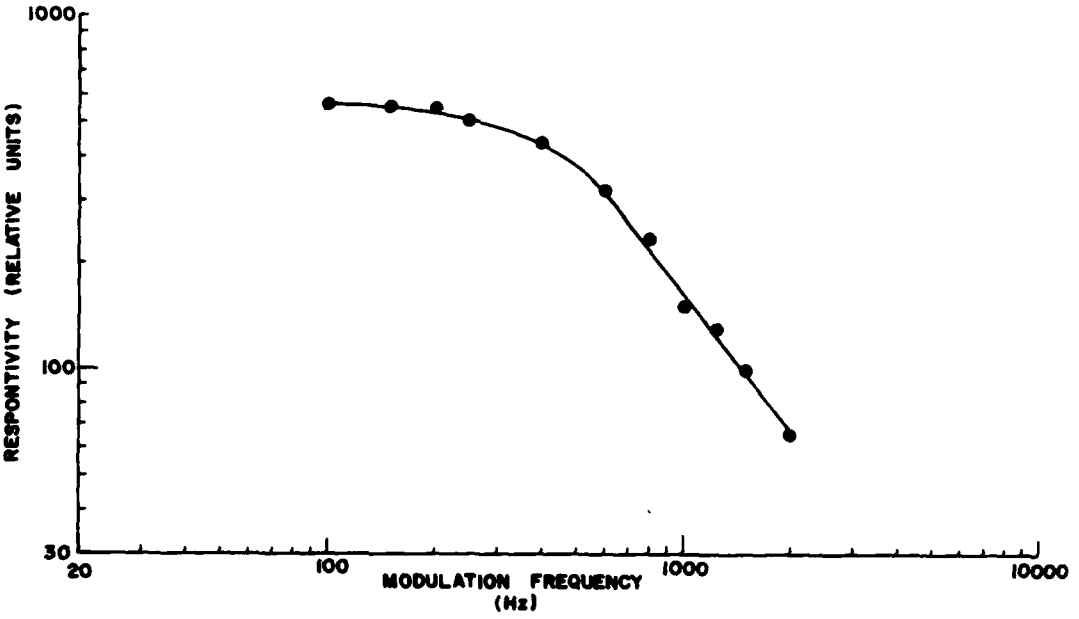

FIGURE 10 - Frequency response of the Stark cell assembly, including the input transformer and the output preamplifier

4.3 Frequency Performance

To evaluate the cell performance, a CO_2 waveguide laser (Ref. 11) was frequency stabilized, by using the previously described Stark cell in a configuration shown in Fig. 11. During the test, the waveguide laser was excited with a power supply (Power Technology) having a 0.5% rms ripple. The lock-in amplifier used in the feedback loop was a Lansing stabilizer, model 80-214. The laser output was combined to a reference signal on a HgCdTe photodiode and it was observed with a frequency counter. This reference laser was a low-pressure CW laser frequency-stabilized on the P(20) line center through standard dithering techniques. The dithering frequency was 510 Hz and the FM deviation amounted to ± 2 MHz. In this test, no particular care was taken to avoid mechanical vibrations, and the frequency stability of the reference laser was not known.

After hard pumping, the Stark cell was filled with a 1:1 mixture of ND_3 and NH_3 to a pressure of 15 torr and it was left to rest for 12 h. The cell was then pumped to 2.5 torr, and the filling valve was closed. A 12-V modulation signal applied to the electrodes, resulted in a maximum modulation of 4 V at the output of the detector. The gain of the input amplifier of the lock-in was set at 20 dB, the feedback loop closed and the dc bias voltage set to obtain a mean beat frequency of 13 MHz. The frequency was monitored with a counter connected to either a calculator or an analog-to-digital converter.

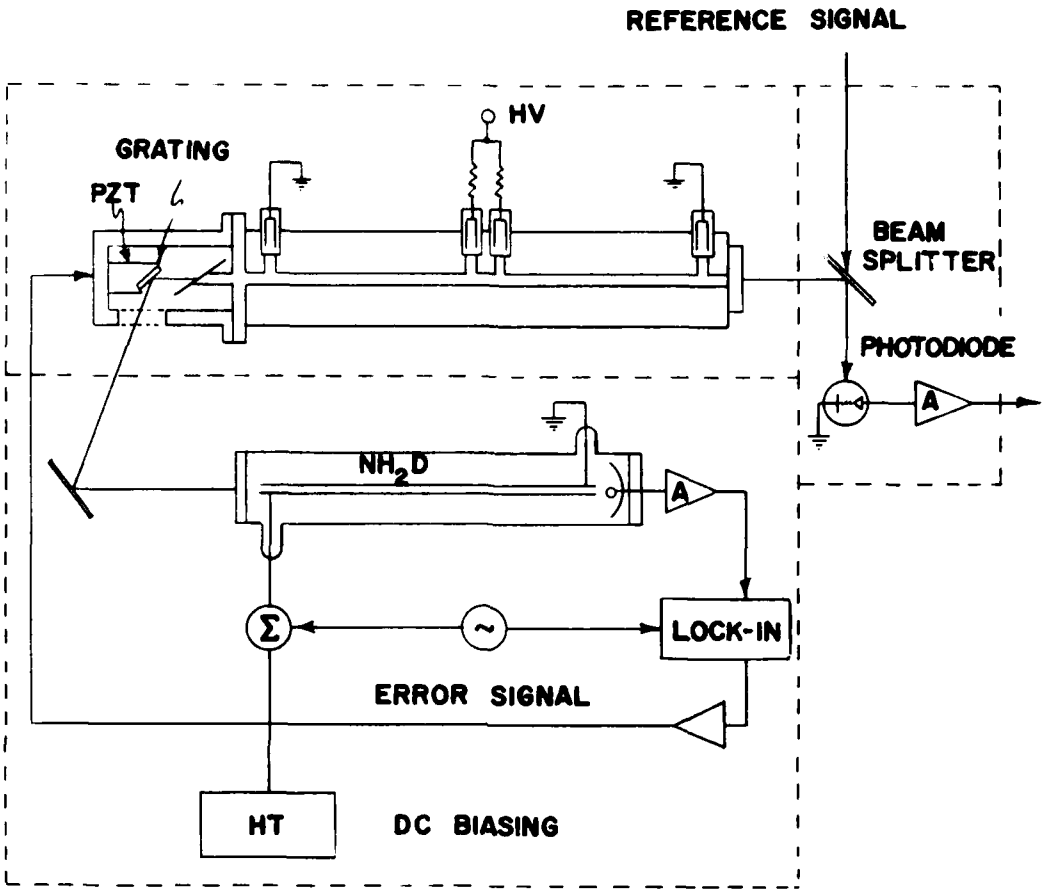

FIGURE 11 - Frequency stability measurement arrangement

A histogram of the probability of occurrence versus the frequency deviation with 1-ms gates shows a standard deviation of about 700 kHz. Figure 12 shows the Allan variance (Ref. 12) of the signal. This result is difficult to interpret but it indicates that it is still possible to improve the short-term stability to reach the white noise regime characterized on such a graph by a slope of -1. The relative contribution of each laser was not determined, but besides mechanical vibrations, some electrical noise sources were identified on both lasers. It was particularly found that both a 120-Hz ripple

on the discharge current of the reference laser and the higher-frequency ripple on the waveguide discharge current contribute to the short-term frequency instability. This contribution has not been evaluated more exactly, as better regulated high voltage sources were not available. However, a more exact evaluation should be obtained by beating together the outputs of two identical lasers both stabilized with Stark cells.

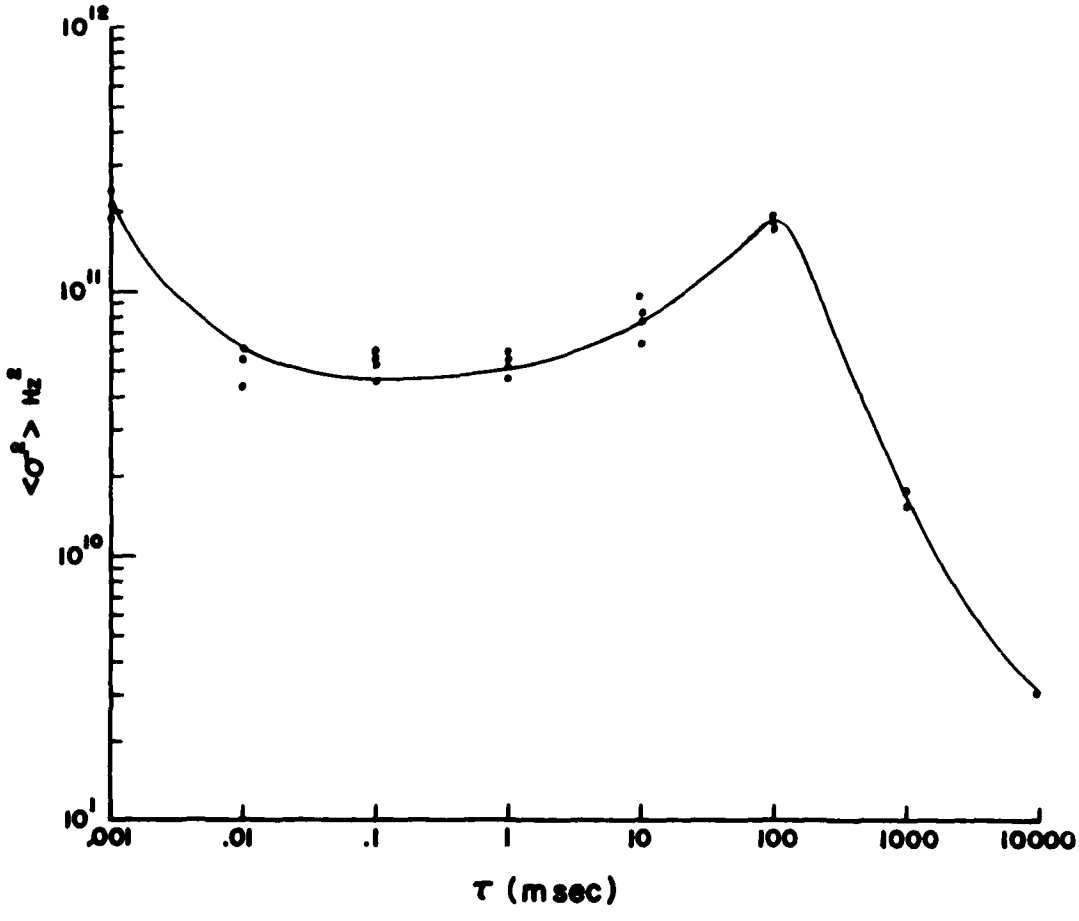

FIGURE 12 - Allan variance of the beat signal

The long-term frequency characteristics were obtained by monitoring the output of the counter over long periods of time. Figure 13, which shows the frequency behavior over such a 2.5-h period, indicates that frequency fluctuations are kept within ± 1.5 MHz. Observation over 5-h periods has also shown fluctuations within these limits when a sufficient warm-up time (≈ 1 hour) was provided to allow the Stark cell bias supply to reach a stable value. Again, it is impossible to determine which laser contributed more strongly to the instability, but it appears that the Stark cell approach is capable of good long-term performance. The spurious frequency jumps that appear from time to time have been related to plasma noise in the reference laser. The characterization of the Stark-cell-stabilized waveguide laser would also require a comparison of two identical sources.

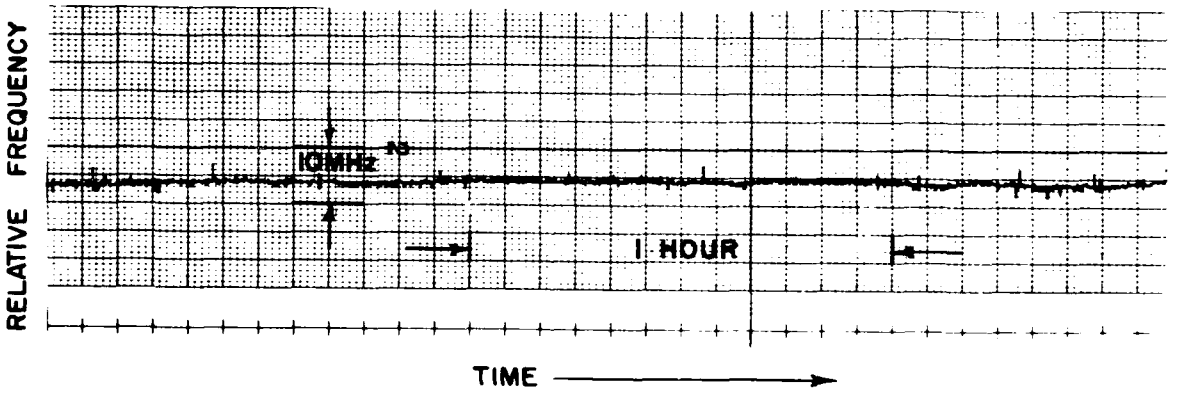

FIGURE 13 - Long-term frequency fluctuations with a frequency offset of 14 MHz

A calibration curve of the Stark cell was finally obtained by reading the beat frequency as a function of the cell bias voltage, as shown in Fig. 14. Since the reference laser is locked to the CO_2 line center, we obtain the frequency relative to the CO_2 P(20) center frequency. The diagram shows that the frequency varies linearly with the bias with a slope of 5.5 ± 0.1 MHz/V over the spanned range and that the resonant voltage amounts to 371 V. The cell must be carefully calibrated in its work position because if it rotated around the propagation axis, it would change the electrical field component along the polarization vector and consequently, it would affect the calibration curve.

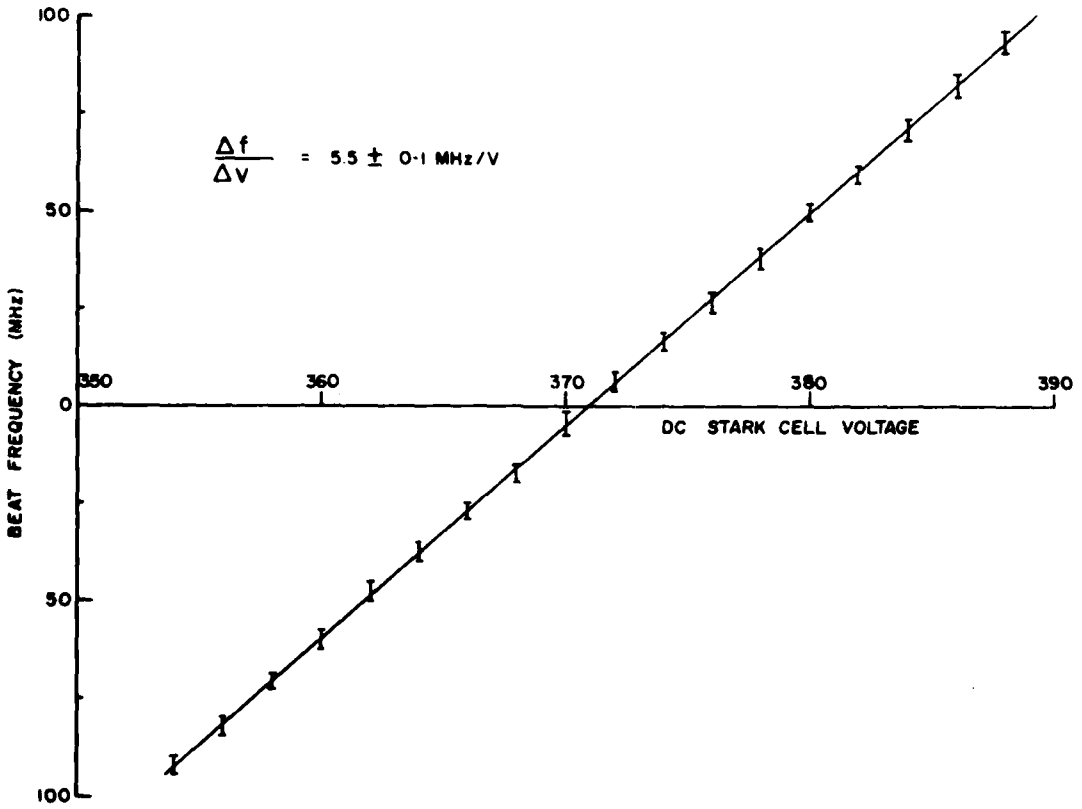

FIGURE 14 - Beat frequency versus dc Stark cell voltage

5.0 CONCLUSION

We have developed a rugged Stark cell that can be used to frequency-lock and tune a CW CO_2 waveguide laser. With that technique, a long-term frequency stability better than ± 1.5 MHz is easily achieved. The laser output is free from the amplitude and frequency modulations inherent to standard cavity dithering stabilization schemes. Furthermore, the laser frequency can easily be tuned by varying the Stark bias voltage. This technique appears suitable for the frequency control of local oscillators in coherent detection systems at 10.6 μm. Since the cell can easily be refilled, new gas can be used to lock onto some other emission lines of the CO_2 laser. If required, the short-term stability could be improved by isolating the laser from mechanical vibrations while the long-term stability would be determined by the feedback gain and the Stark bias voltage regulation.

6.0 ACKNOWLEDGEMENTS

The authors thank Mr. P. Noreau, who realized the mechanical design of the cell, and Dr. P. Pace, who took the Allan variance data, for their invaluable help. Many stimulating discussions with Mr. J. Cruickshank, Dr. G. Otis and Dr. D. Vincent are also acknowledged.

7.0 REFERENCES

1. Nussmeier, T.A. and Abrams, R.L., "Stark Cell Stabilization of CO_2 Lasers", Appl. Phys. Lett., Vol. 25, pp. 615-617, 1974.

2. Jensen, R.E. and Tokin, M.S., "An Investigation of Gases for Stark Modulating the CO_2 Laser", IEEE J. Quant. Electron., Vol. QE-8, pp. 64-68, 1972.

3. Martin, J.M., Corcoran, J.V. and Smith, W.T., "Identification of Absorption Lines in Gases Used to Modulate the CO_2 Laser", IEEE J. Quant. Electron., Vol. QE-10, pp. 191-195, 1974.

4. Brewer, R.G., Kelly, M.J. and Javan, A., "Precision Infrared Stark Spectra of $N^{14}H_2D$ Using Lamb Dip", Phys. Rev. Lett., Vol. 23, pp. 559-563, 1969.

5. Kelly, M.J., Francke, R.E. and Feld, M.S., "Rotational-Vibrational Spectroscopy of NH_2D Using High Resolution Laser Techniques", J. Chem. Phys., Vol. 53, pp. 2979-2980, 1970.

6. Plant, T.K. and Abrams, R.L., "Broadening and Absorption Coefficients in $N^{14}H_2D$", J. Appl. Phys. (USA), Vol. 47, pp. 4006-4008, 1976.

7. Tangonan, G.L. and Abrams, R.L., "Stark-Tuned Resonances of $N^{15}H_2D$ with CO_2 Laser Lines", Appl. Phys. Lett., Vol. 29, pp. 179-181, 1976.

8. Asowa, C.K. and Plant, T.K., "Wideband Modulation of the $C^{13}O_2^{16}$ Laser R(18) Line at 10.784 μm with an $N_{14}H_3$ Stark Cell", Appl. Phys. Lett., Vol. 30, pp. 96-98, 1977.

9. Cobine, J.D., "Gaseous Conductors, Theory and Engineering Applications", Dover Publications Inc., New York, 1958.

10. Johnston, A.R. and Melville, R.D.S. Jr., "Stark-Effect Modulation of a CO_2 Laser by NH_2D", Appl. Phys. Lett., Vol. 19, pp. 503-506, 1971.

11. Lavigne, P., Otis, G. and Vincent, D., "Performance Characteristics of a CO_2 Waveguide Laser", DREV R-4150/79, August 1979, UNCLASSIFIED

12. Allan, W.D., "Statistics of Atomic Frequency Standards", Proc. IEEE, Vol. 54, pp. 221-230, 1966.

CRDV R-4188/80 (NON CLASSIFIE)

Bureau - Recherche et Développement, MDN, Canada.
CRDV, C.P. 8800, Courcelette, Qué. G0A 1R0

"Une cellule de Stark pour contrôler la fréquence d'un laser CO_2 à guide d'ondes"
par P. Lavigne, A. Deslauriers et J. Lemay

Dans ce rapport, nous décrivons le mode d'opération et les détails de construction d'une cellule à effet Stark, susceptible de contrôler la fréquence d'un oscillateur local à 10 µm, et nous en analysons les caractéristiques. Avec cette cellule, nous avons réussi à syntoniser un laser CO_2 continu à guide d'ondes dans un domaine de fréquence de ± 100 MHz autour du centre de la raie P(20) du CO_2, à 10.6 µm, et nous avons obtenu une stabilité à long terme supérieure à ± 1.5 MHz. (NC)

CRDV R-4188/80 (NON CLASSIFIE)

Bureau - Recherche et Développement, MDN, Canada.
CRDV, C.P. 8800, Courcelette, Qué. G0A 1R0

"Une cellule de Stark pour contrôler la fréquence d'un laser CO_2 à guide d'ondes"
par P. Lavigne, A. Deslauriers et J. Lemay

Dans ce rapport, nous décrivons le mode d'opération et les détails de construction d'une cellule à effet Stark, susceptible de contrôler la fréquence d'un oscillateur local à 10 µm, et nous en analysons les caractéristiques. Avec cette cellule, nous avons réussi à syntoniser un laser CO_2 continu à guide d'ondes dans un domaine de fréquence de ± 100 MHz autour du centre de la raie P(20) du CO_2, à 10.6 µm, et nous avons obtenu une stabilité à long terme supérieure à ± 1.5 MHz. (NC)

CRDV R-4188/80 (NON CLASSIFIE)

Bureau - Recherche et Développement, MDN, Canada.
CRDV, C.P. 8800, Courcelette, Qué. G0A 1R0

"Une cellule de Stark pour contrôler la fréquence d'un laser CO_2 à guide d'ondes"
par P. Lavigne, A. Deslauriers et J. Lemay

Dans ce rapport, nous décrivons le mode d'opération et les détails de construction d'une cellule à effet Stark, susceptible de contrôler la fréquence d'un oscillateur local à 10 µm, et nous en analysons les caractéristiques. Avec cette cellule, nous avons réussi à syntoniser un laser CO_2 continu à guide d'ondes dans un domaine de fréquence de ± 100 MHz autour du centre de la raie P(20) du CO_2, à 10.6 µm, et nous avons obtenu une stabilité à long terme supérieure à ± 1.5 MHz. (NC)

CRDV R-4188/80 (NON CLASSIFIE)

Bureau - Recherche et Développement, MDN, Canada.
CRDV, C.P. 8800, Courcelette, Qué. G0A 1R0

"Une cellule de Stark pour contrôler la fréquence d'un laser CO_2 à guide d'ondes"
par P. Lavigne, A. Deslauriers et J. Lemay

Dans ce rapport, nous décrivons le mode d'opération et les détails de construction d'une cellule à effet Stark, susceptible de contrôler la fréquence d'un oscillateur local à 10 µm, et nous en analysons les caractéristiques. Avec cette cellule, nous avons réussi à syntoniser un laser CO_2 continu à guide d'ondes dans un domaine de fréquence de ± 100 MHz autour du centre de la raie P(20) du CO_2, à 10.6 µm, et nous avons obtenu une stabilité à long terme supérieure à ± 1.5 MHz. (NC)

DREV R-4188/80 (UNCLASSIFIED)

Research and Development Branch, DND, Canada.
DREV, P.O. Box 8800, Courcelette, Que. GOA 1RO

"A Stark Cell for Frequency Control of a Waveguide CO_2 Laser"
by P. Lavigne, A. Deslauriers and J. Lemay

In this report, we describe the mode of operation and the design of a Stark cell suitable for the frequency control of a local oscillator at 10 μm, and we analyze its characteristics. Using this cell, a waveguide CW CO_2 laser was tuned over ± 100 MHz around the line center of the P(20) CO_2 line, at 10.6 μm, and a long-term frequency stability better than ± 1.5 MHz was achieved. (U)

DREV R-4188/80 (UNCLASSIFIED)

Research and Development Branch, DND, Canada.
DREV, P.O. Box 8800, Courcelette, Que. GOA 1RO

"A Stark Cell for Frequency Control of a Waveguide CO_2 Laser"
by P. Lavigne, A. Deslauriers and J. Lemay

In this report, we describe the mode of operation and the design of a Stark cell suitable for the frequency control of a local oscillator at 10 μm, and we analyze its characteristics. Using this cell, a waveguide CW CO_2 laser was tuned over ± 100 MHz around the line center of the P(20) CO_2 line, at 10.6 μm, and a long-term frequency stability better than ± 1.5 MHz was achieved. (U)

DREV R-4188/80 (UNCLASSIFIED)

Research and Development Branch, DND, Canada.
DREV, P.O. Box 8800, Courcelette, Que. GOA 1RO

"A Stark Cell for Frequency Control of a Waveguide CO_2 Laser"
by P. Lavigne, A. Deslauriers and J. Lemay

In this report, we describe the mode of operation and the design of a Stark cell suitable for the frequency control of a local oscillator at 10 μm, and we analyze its characteristics. Using this cell, a waveguide CW CO_2 laser was tuned over ± 100 MHz around the line center of the P(20) CO_2 line, at 10.6 μm, and a long-term frequency stability better than ± 1.5 MHz was achieved. (U)

DREV R-4188/80 (UNCLASSIFIED)

Research and Development Branch, DND, Canada.
DREV, P.O. Box 8800, Courcelette, Que. GOA 1RO

"A Stark Cell for Frequency Control of a Waveguide CO_2 Laser"
by P. Lavigne, A. Deslauriers and J. Lemay

In this report, we describe the mode of operation and the design of a Stark cell suitable for the frequency control of a local oscillator at 10 μm, and we analyze its characteristics. Using this cell, a waveguide CW CO_2 laser was tuned over ± 100 MHz around the line center of the P(20) CO_2 line, at 10.6 μm, and a long-term frequency stability better than ± 1.5 MHz was achieved. (U)


DA
FILM